Effect of Streptavidins with Varying Biotin Binding Affinities on the Properties of Biotinylated Gramicidin Channels†

Y. N. Antonenko,*,‡ T. I. Rokitskaya,‡ E. A. Kotova,‡ G. O. Reznik,§ T. Sano,|| and C. R. Cantor§

Belozersky Institute, Moscow State University, Moscow 119992, Russia, Center for Advanced Biotechnology and Department of Biomedical Engineering, Boston University, Boston, Massachusetts 02215, and Center for Molecular Imaging, Diagnosis and Therapy and Basic Science Laboratory, Department of Radiology, Beth Israel Deaconess Medical Center, Harvard Medical School, Boston, Massachusetts 02215

Received June 9, 2003; Revised Manuscript Received February 5, 2004

ABSTRACT: The pentadecapeptide gramicidin A, which is known to form highly conductive ion channels in a bilayer lipid membrane by assembling as transmembrane head-to-head dimers, can be modified by attaching a biotin group to its C-terminus through an aminocaproyl spacer. Such biotinylated gramicidin A analogues also form ion channels in a hydrophobic lipid bilayer, exposing the biotin group to the aqueous bathing solution. Interaction of the biotinylated gramicidin channels with (strept)avidin has previously been shown to result in the appearance of a long-lasting open state with a doubled transition amplitude in single-channel traces and a deceleration of the macroscopic current kinetics as studied by the sensitized photoinactivation method. Here this interaction was studied further by using streptavidin mutants with weakened biotin binding affinities. The Stv-F120 mutant, having a substantially reduced biotin binding affinity, exhibited an efficacy similar to that of natural streptavidin in inducing both double-conductance channel formation and deceleration of the photoinactivation kinetics of the biotinylated gramicidin having a long linker arm. The Stv-A23D27 mutant with a severely weakened biotin binding affinity was ineffective in eliciting the double-conductance channels, but decelerated noticeably the photoinactivation kinetics of the long linker biotinylated gramicidin. However, the marked difference in the effects of the mutant and natural streptavidins was smaller than expected on the basis of the substantially reduced biotin binding affinity of the Stv-A23D27 mutant. This may suggest direct interaction of this mutant streptavidin with a lipid membrane in the process of its binding to biotinylated gramicidin channels. The role of linker arm length in the interaction of biotinylated gramicidins with streptavidin was revealed in experiments with a short linker gramicidin. This gramicidin analogue appeared to be unable to form double-conductance channels, though several lines of evidence were indicative of its binding by streptavidin. The data obtained show the conditions under which the interaction of streptavidin with biotinylated gramicidin leads to the formation of the double-conductance tandem channels composed of two cross-linked transmembrane dimers.

Recording of electrical currents flowing through proteinaceous channels in lipid membranes has recently become a powerful tool for monitoring single molecular recognition events due to its extremely high sensitivity (*1*, *2*). The fact that each specific binding event results in opening or closing of a certain ion channel makes such systems very attractive for studying receptor−ligand interaction at the membrane surface. The crucial step of such interactions is the binding of ligands to membrane receptors, which differs substantially from their binding to proteins in solution, as evidenced by studies using self-assembled monolayers (*3*, *4*) and Langmuir−Blodgett films (*5*). A series of studies has shown that the binding of streptavidin to surfaces bearing covalently bound biotin groups at different surface densities is rather sophisticated; e.g., it exhibits cooperativity and shows additional protein−protein and protein−surface interactions (*4*−*7*).

Governing processes of ion channel gating via ligand binding is of potential interest as a prototype of efficient biosensors. The mechanisms of the channel nanodevices proposed so far are based on either the regulation of ion passage through the channel interior of relatively large pores, such as those formed by α-hemolysin (*8*), or the extramembrane control of channel peptide assembly and/or dissociation of smaller pores formed by gramicidin A (*9*−*11*) or alamethicin (*12*, *13*), eventually leading to channel current modulation. The mobility of channel-forming molecules in the lipid bilayer is thought to contribute substantially (*9*) to the process of conducting state assembly of biotinylated gramicidin channels, which have been used in the construction of a series of biosensors (*14*) because of their ability to interact with biotin-binding proteins such as streptavidin and avidin. The (strept)-avidin−biotin system, utilized in these biosensors, offers a wide range of biotechnological and general research applica-

† This work was partially supported by Grants 03-04-48905 and 03-04-06151 from the Russian Foundation for Basic Research.

* To whom correspondence should be addressed: Belozersky Institute of Physico-Chemical Biology, Moscow State University, Moscow 119992, Russia. Fax: +(70-95)-939-31-81. E-mail: antonen@genebee.msu.su.

‡ Moscow State University.

§ Boston University.

|| Harvard Medical School.

10.1021/bi034984r CCC: $27.50
Published on Web 03/17/2004

tions (*15*) and has served as the subject of a series of studies aimed at exploring the mechanisms of tight protein−ligand interactions (reviewed in refs *16* and *17*; see also ref *18*). Several successful attempts to modulate the biotin binding affinity by site-directed mutagenesis have become especially important (*19*−*27*).

Since the pioneering work of Cornell et al. (*9*), there have been a few studies on the interaction of (strept)avidin with channels formed by biotinylated gramicidin analogues (*28*−*30*). At present, the mechanism of the effect of (strept)avidin on these channels remains obscure. In the previous work (*31*), we presented evidence that the binding of (strept)avidin induces the formation of a new type of a tandem gramicidin channel composed of two synchronously functioning channels. Here, the interaction between biotinylated gramicidins and streptavidins with varying biotin binding affinities was studied at both the macroscopic and single-channel levels to understand how the binding affinity and steric factors determine the mode of the interaction. In particular, we studied the effect of streptavidin mutants Stv-F120 and Stv-A23D27, in which the biotin binding affinities (K_a) were reduced from approximately 10^{15} M^{-1}, characteristic of natural streptavidin (*32*, *33*), to approximately 10^8−10^9 and 10^4 M^{-1}, respectively (*19*, *22*).

MATERIALS AND METHODS

BLMs[1] were formed from a 2% solution of diphytanoylphosphatidylcholine (DPhPC, Avanti Polar Lipids, Alabaster, AL) in *n*-decane (Merck, Darmstadt, Germany) by the brush technique on a hole in a Teflon partition separating two compartments of a cell containing aqueous buffer solutions. A cell with a 0.15 mm diameter hole was used in single-channel experiments, and one with a 0.55 mm diameter hole was used in photoinactivation experiments. The biotinylated analogues of gramicidin A (generous gifts of F. Separovic, University of Melbourne, Melbourne, Australia) with a biotin group attached to the C-terminus of gramicidin A through a linker arm comprising five (gA5XB) or two (gA2XB) aminocaproyl groups were added from stock solutions in ethanol to the bathing solutions at both sides of the BLM and incubated for 15 min with constant stirring. The addition of the channel former at a concentration of ~1 nM induced a current across the BLM of the order of 1 μA. The structure and synthesis of biotinylated gramicidins were described previously (*34*, *35*). Natural streptavidin (Stv) and biotin were from Fluka (Buchs, Switzerland). Two streptavidin mutants, Stv-F120 (also called Stv-38) (*19*) and Stv-A23D27 (*22*), were obtained as described previously (*19*, *22*). In all experiments, the solution that was used consisted of 1 M KCl, 10 mM Tris, 10 mM MES, and 10 mM β-alanine (pH 7.0). In photoinactivation experiments, aluminum trisulfophthalocyanine ($AlPcS_3$) from Porphyrin Products (Logan, UT) was added to the bathing solution on the *trans* side (the *cis* side is the front side with respect to the flash lamp). All experiments were carried out at room temperature (22−24 °C).

[1] Abbreviations: DPhPC, diphytanoylphosphatidylcholine; gA, gramicidin A; gA5XB, gA with a biotin group covalently attached to the C-terminus of gA through a linker arm comprising five aminocaproyl groups; gA2XB, gA with a biotin group covalently attached to the C-terminus of gA through a linker arm comprising two aminocaproyl groups; Stv, streptavidin; $AlPcS_3$, aluminum trisulfophthalocyanine; BLM, bilayer lipid membrane; Tris, tris(hydroxymethyl)aminomethane; MES, 4-morpholineethanesulfonic acid.

Electric currents (I) were recorded under voltage-clamp conditions. Voltages were applied to BLMs with Ag−AgCl electrodes placed directly into the cell. The currents, measured by means of a patch-clamp amplifier (OES-2, OPUS, Moscow, Russia) in single-channel experiments and by a U5-11 amplifier in photoinactivation experiments, were digitized by using a LabPC 1200 computer (National Instruments, Austin, TX) and analyzed using a personal computer with the help of WinWCP Strathclyde Electrophysiology Software designed by J. Dempster (University of Strathclyde, Strathclyde, U.K.). Single-channel currents were low-pass filtered with a cutoff frequency of 100 Hz, sampled at 1 kHz, and stored directly on a hard disk. A low-pass digital filter with a cutoff frequency of 53 Hz was used in the recordings.

In photoinactivation experiments, BLMs were illuminated by single flashes produced by a xenon lamp with flash energy of ~400 mJ/cm^2 and a flash duration of <2 ms. The time course of a decrease in the macroscopic gramicidin-mediated current (I) across a BLM provoked by a flash in the presence of a photosensitizer [e.g., aluminum trisulfophthalocyanine ($AlPcS_3$)] was measured. The sensitized photoinactivation is associated with damage to tryptophan residues in gramicidin, caused by light-induced generation of reactive oxygen species (*36*−*38*). As shown previously (*39*), the time course of the flash-induced current decrease (the current transient called here the photoinactivation kinetics) reflects the equilibration of gramicidin dimer and monomer concentrations after a concentration jump caused by damage to a fraction of the gramicidin molecules. The time course of the decrease in the current is, at a first approximation, a monoexponential function of time

$$I(t) = (I_0 - I_\infty) \exp(-t/\tau) + I_\infty$$

where I_0, I_∞, and τ are the initial current prior to illumination, the steady state level of the current established as a result of relaxation after the flash, and the characteristic time of photoinactivation, respectively. The characteristic time of photoinactivation (τ) derived from the exponential approximation of the current transient (an exponential factor of a monoexponential curve fitting the time course) has been shown to correspond to the gramicidin channel lifetime. Another parameter of the light-induced current transient, the relative amplitude of photoinactivation [$\alpha = (I_0 - I_\infty)/I_0$], is determined by the amount of the reactive oxygen species generated upon excitation of the photosensitizer by a light flash (*40*). Because the light-induced decrease in the gramicidin-mediated current is due to the reduction of the number of open channels (*37*, *38*), α is equal to the fraction of damaged gramicidin channels.

The gA5XB photoinactivation kinetics recorded after the addition of different streptavidins were poorly fitted by a monoexponential curve, but were described well by a sum of two exponentials

$$(I - I_\infty)/(I_0 - I_\infty) = \beta_1 \exp(-t/\tau_1) + \beta_2 \exp(-t/\tau_2)$$

where $\beta_1 + \beta_2 = 1$. Under these conditions, the photoinactivation kinetics were characterized by three parameters, τ_1, τ_2, and β_2. In most cases, the value of τ_1 practically coincided with the value of τ measured in control experiments, in the absence of streptavidin, and amounted to 3.5−5 s at room

temperature. Therefore, two parameters, β_2 and τ_2, were sufficient to characterize the photoinactivation kinetics observed in the presence of different streptavidins. In general, the characteristic time of photoinactivation depends on the magnitude of the macroscopic current that is determined by the surface density of gramicidin molecules (*39*). However, measurements made in the presence of streptavidin have shown that β_2 and τ_2 were practically independent of the current within the range of 0.1−3 μA, when a voltage of 50 mV was applied to a BLM.

RESULTS

Previously, we have shown (*31*) that the addition of streptavidin to the bathing solutions of a BLM provokes the appearance of an extremely stable state of ionic channels formed by gA5XB (biotinylated gramicidin with a long linker arm comprising five aminocaproyl groups) that is characterized by an approximately doubled transition amplitude (double-conductance channel). In the study presented here, we compare the effects of streptavidins with varying biotin binding affinities on the channel properties of gA5XB.

Figure 1 illustrates single-channel recordings of gA5XB after the incubation with natural streptavidin (Stv) (trace A), and two mutants with reduced biotin binding affinities, Stv-F120 (*19*) (trace B) and Stv-A23D27 (*22*) (trace C), added to both sides of the BLM. As described in our earlier paper (*29*), in the absence of Stv gA5XB exhibits current fluctuations similar to those of gramicidin A with a single-channel conductance of 17.6 ± 1 pS. The single-channel lifetime histogram of gA5XB displays a single-exponential decay distribution with an exponential factor of 3.6 s (*29*). Stv-F120, like Stv, suppressed the usual current fluctuations of gA5XB and induced the transition to a very long-lived open state with the single-channel conductance exceeding that of the control more than 2-fold (40.2 ± 3 pS). In contrast, the formation of the long-lived double-conductance channel was not observed with Stv-A23D27.

Fast fluctuations of the current generally preceding the opening of the double-conductance channels of gA5XB after the addition of Stv (Figure 2A; see also ref *31*) were also recorded with Stv-F120 (Figure 2B). However, similar bursts of very short-lived channel events having the transition amplitude coinciding with that of the control single channels of gA5XB were also elicited by the addition of Stv-A23D27 (Figure 2C), though this mutant did not induce the long-lasting double-conductance state in the single-channel traces. With Stv-A23D27, these bursts occurred rarely, as compared to Stv and Stv-F120 (Figure 1). The open state duration of individual events in these bursts displayed an exponential distribution with exponential factors of 60 ± 10, 43 ± 3, and 32 ± 6 ms for Stv, Stv-F120, and Stv-A23D27, respectively. With Stv, the bursts, lasting for an average of 100 s, were usually terminated by the emergence of the double-conductance channels. On the contrary, with Stv-F120, only some of the bursts were stopped by the formation of the long-lived double-conductance channel state, while the others lasted on average 27 ± 10 s. For Stv-A23D27, the average total duration of the bursts was 12 ± 5 s. Apparently, the value of 100 s can be considered the lower limit for the duration of the gA5XB current bursts induced by Stv. It is of interest that similar fast fluctuations of the single-channel current were observed after the addition of Stv also in the case of gA2XB (a biotinylated gramicidin analogue with a short linker arm) that did not form the double-conductance channels in our single-channel experiments (*31*). The gA2XB bursts were characterized by the 33 ± 4 ms open state and the 140 ± 30 s average total duration.

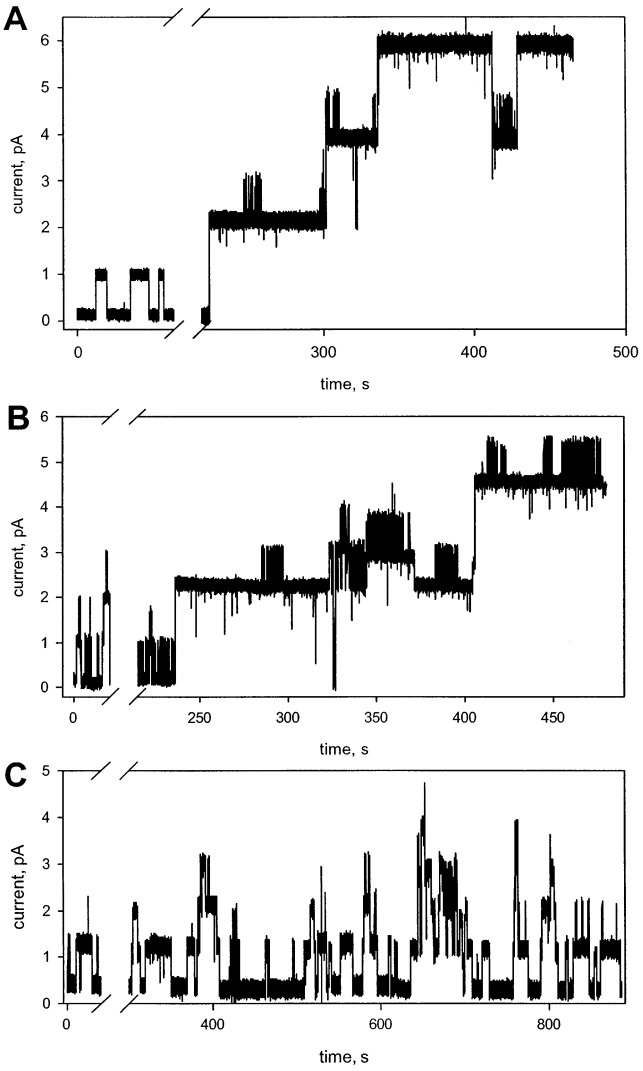

FIGURE 1: Single-channel traces of gA5XB in the absence (shown before the break) and presence of 20 nM Stv (A), 20 nM Stv-F120 (B), or 20 nM Stv-A23D27 (C) (shown after the break). The BLM voltage was 50 mV. The solution consisted of 1 M KCl, 10 mM Tris, 10 mM MES, and 10 mM β-alanine (pH 7.0). Planar bilayers were from DPhPC.

The binding of multivalent ligands such as streptavidin to surfaces depends essentially on the surface density of receptors, i.e., biotin groups (*4*). To estimate the effect of streptavidins on the open state duration of gA5XB channels at much higher surface densities of gA5XB, we employed the method of sensitized photoinactivation (*37*, *38*). Figure 3 demonstrates the effect of Stv-F120 (curve 3) and Stv-A23D27 (curve 4) on gA5XB photoinactivation kinetics, as compared to that of Stv (curve 2). The control photoinactivation kinetics of gA5XB measured in the absence of streptavidin were fitted well by a monoexponential curve with a characteristic time of 3.7 s (curve 1). The normalized photoinactivation kinetics (Figure 3A inset) reveal that the addition of Stv-F120 led to a dramatic deceleration of the gA5XB photoinactivation kinetics, similar to the effect of

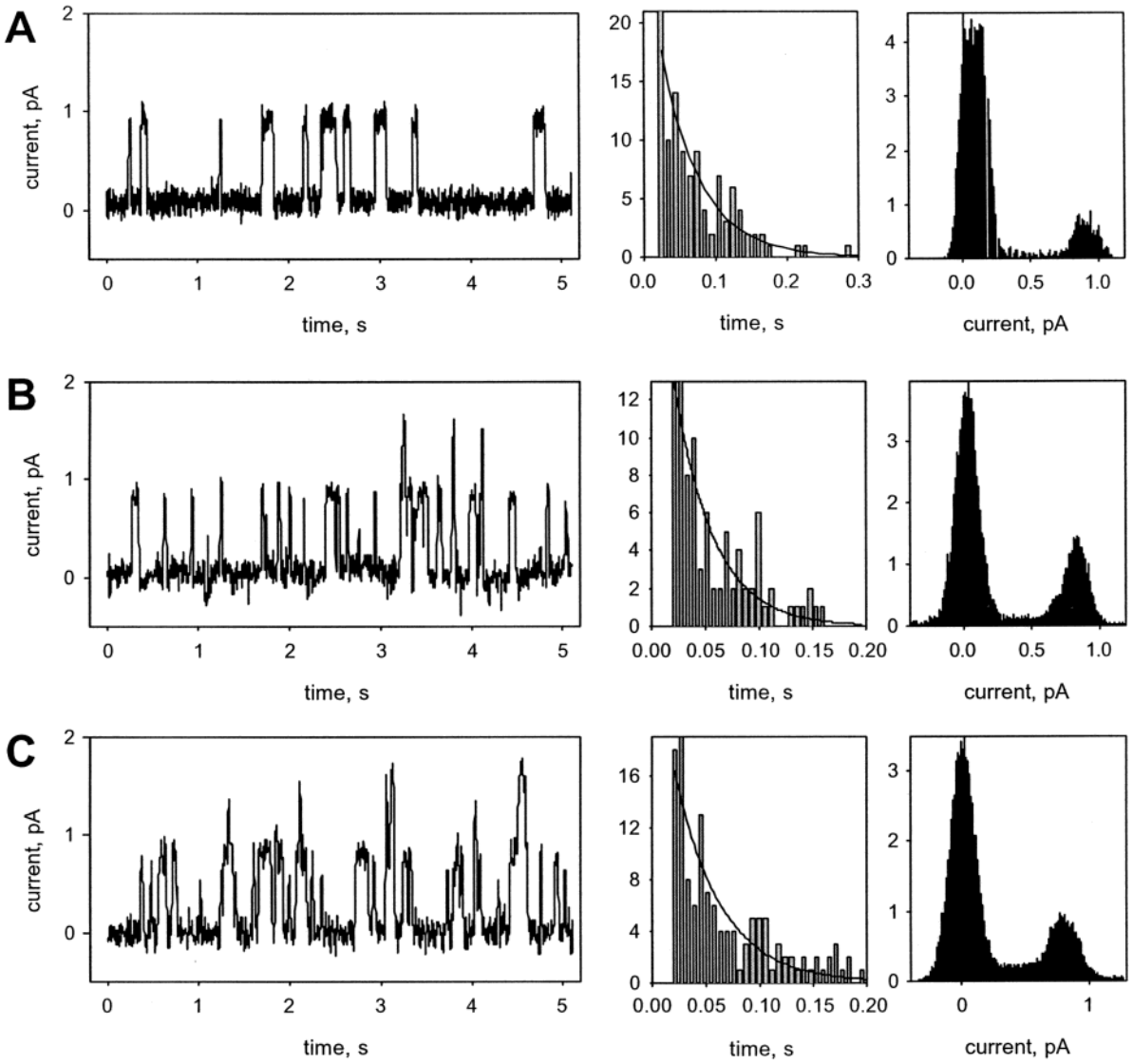

FIGURE 2: Fast fluctuations of the gA5XB single-channel current after the addition of 20 nM Stv (A), 20 nM Stv-F120 (B), or 20 nM Stv-A23D27 (C) to both sides of the BLM observed prior to the appearance of the events shown in Figure 1. The middle column shows the open state duration histograms with the exponential fits (the exponential factor is 55 ms for Stv, 42 ms for Stv-F120, and 36 ms for Stv-A23D27). The right column shows the corresponding current amplitude histograms. The BLM voltage was 50 mV. The solution was the same as that described in the legend of Figure 1. Planar bilayers were from DPhPC.

Stv (*31*) and avidin (*29*). All of the gA5XB photoinactivation kinetics measured in the presence of streptavidins were fitted well by a biexponential curve

$$(I - I_\infty)/(I_0 - I_\infty) = \beta_1 \exp(-t/\tau_1) + \beta_2 \exp(-t/\tau_2)$$

Importantly, the exponential component with parameters β_2 and τ_2 (below called the slow phase of photoinactivation) appeared to make the predominant contribution to the photoinactivation kinetics not only in the presence of Stv and Stv-F120 but also in the presence of Stv-A23D27. Figure 3B compares the values of τ_2 and β_2, when different streptavidins were used, with the control parameters (τ and β, taken to be 100%) of the kinetics measured in the absence of streptavidin. Stv-A23D27 at a concentration of 20 nM also induced the deceleration of the gA5XB photoinactivation kinetics, though it was less pronounced than with Stv and Stv-F120. The addition of biotin to the bathing solutions prior to the addition of streptavidins completely prevented the effect of Stv and its mutants as expected (data not shown).

Thus, at a high surface density of biotin groups, the significant lengthening of the gA5XB open channel state occurred in the presence of all of the streptavidins that were tested, including Stv-A23D27. Table 1 presents the concentration dependence of the effect of Stv and its mutants. At a concentration of 20 nM, the effect of all of the streptavidins that were studied became saturated. In addition, the concentrations at which the effect of different streptavidins became pronounced differed by only 2 orders of magnitude (0.2 nM for Stv and Stv-F120 and 20 nM for Stv-A23D27), although the biotin binding affinities of these mutants differ by approximately 11 orders of magnitude.

Our earlier study has shown that the addition of excess free biotin to the bathing solutions removes the decelerating effect of avidin on the gA5XB photoinactivation kinetics (*29*). Figure 4 demonstrates that the addition of biotin at 20 μM almost completely abolished the decelerating effect of Stv, partially removed the effect of Stv-F120, and was much less effective with Stv-A23D27. To estimate the degree of the decelerating effect in these experiments, we used the

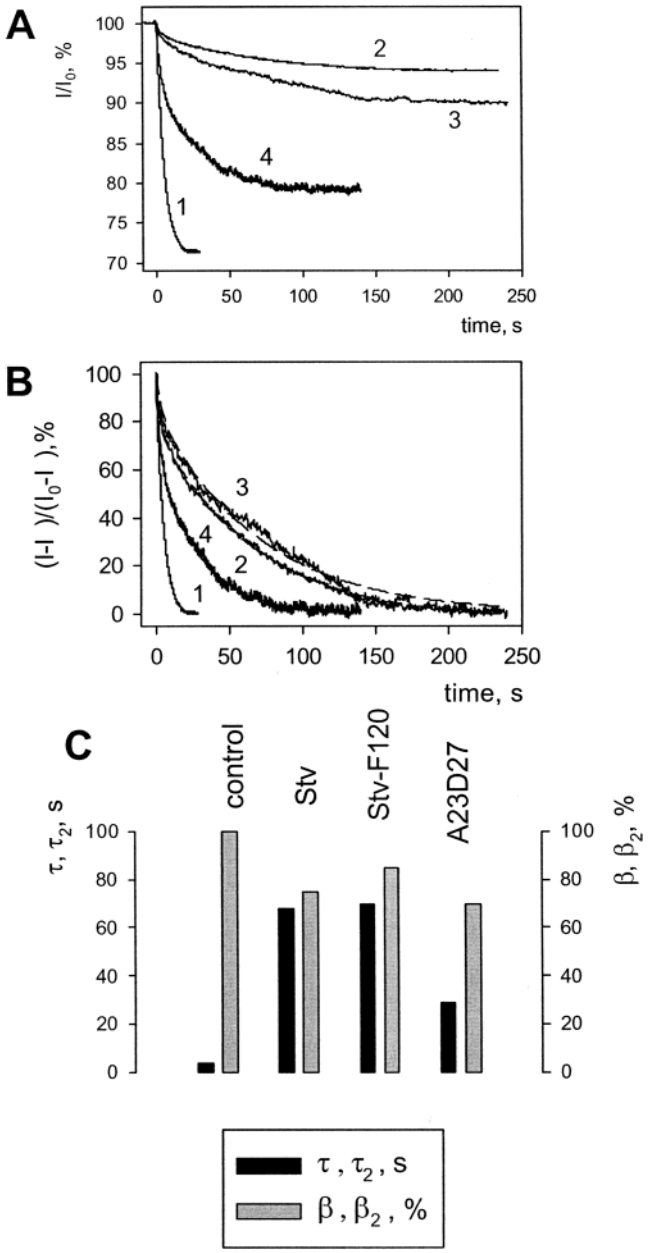

FIGURE 3: (A) Time courses of the decrease in the gA5XB-mediated current across a BLM after a flash of visible light (at time zero) in the presence of 1 μM $AlPcS_3$ before (curve 1) and after the addition of 20 nM Stv (curve 2), 20 nM Stv-F120 (curve 3), or 20 nM Stv-A23D27 (curve 4). The normalized values of the current (I/I_0) are plotted vs time. The initial current (I_0) was approximately 1 μA. The BLM voltage was 50 mV. The solution was the same as that described in the legend of Figure 1. (B) The same data from panel A are replotted as $(I - I_\infty)/(I_0 - I_\infty)$ vs time. Dashed curves are best fits plotted according to the equation $(I - I_\infty)/(I_0 - I_\infty) = \beta_1 \exp(-t/\tau_1) + \beta_2 \exp(-t/\tau_2)$, with the corresponding parameters (β_2 and τ_2) presented in panel C, as compared to the control values of τ and β for gA5XB without streptavidin that are shown at the left side of the chart.

monoexponential approximation for all of the curves and compared the mean values (τ_m) of the characteristic time of photoinactivation thus obtained.

Figure 5 displays the temperature dependence of the characteristic time (τ) of gA5XB photoinactivation in the control and that of τ_2 in the presence of Stv. A small difference in the slopes of the two temperature dependences in Arrhenius coordinates suggests that the activation energy

Table 1: Concentration Dependence of the Effects of Streptavidins on the Photoinactivation Kinetics of gA5XB[a]

protein	concn (nM)	$\beta_1 = 1 - \beta_2$ (%)	τ_1 (s)	β_2 (%)	τ_2 (s)
Stv	0.02	100	4.8 ± 0.5	0	–
	0.2	55	5.0 ± 0.3	45 ± 3	56 ± 5
	2	40	5.3 ± 1.1	60 ± 10	70 ± 11
	20	12	4.3 ± 0.6	73 ± 4	88 ± 13
Stv-F120	0.02	100	5.5	0	–
	0.2	38	3.8 ± 0.8	62 ± 5	41 ± 15
	2	28	3.5 ± 0.4	71 ± 6	72 ± 20
	20	33	4.1 ± 1.5	68 ± 4	70 ± 10
Stv-A23D27	2	100	5.6 ± 0.4	0	–
	20	39	5.7 ± 0.5	61 ± 5	44 ± 10
	100	38	8.0 ± 1.5	62 ± 4	103 ± 9

[a] The conditions were the same as in the legend of Figure 3.

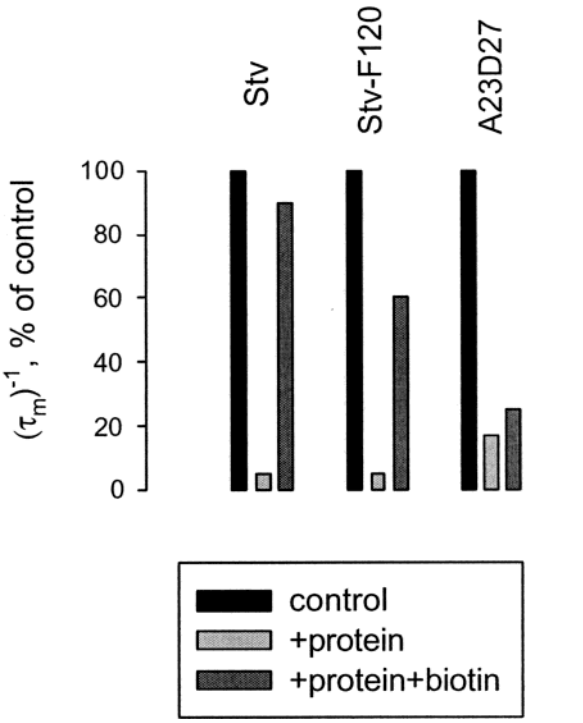

FIGURE 4: Effect of biotin (20 μM), added after 20 nM Stv (left), 20 nM Stv-F120 (middle), or 20 nM Stv-A23D27 (right), on the mean value of the characteristic time (τ_m) calculated from the monoexponential approximation of gA5XB photoinactivation kinetics. The control value of τ_m^{-1}, corresponding to τ^{-1} for gA5XB without streptavidin, is taken to be 100%.

changed only slightly (from 23.7 to 20.6 kcal/mol) upon addition of Stv. On the basis of these data, the addition of Stv may be considered to be equivalent to a decrease in temperature of ~30 °C. The temperature dependence of the characteristic time of photoinactivation of gA5XB (Figure 5) proved to be similar to that of gA studied earlier (*39*). Namely, both gA and gA5XB exhibited a marked reduction in τ upon increasing the temperature with rather close values of the activation energy (22 and 23.7 kcal/mol for gA and gA5XB, respectively).

To gain insight into the possible involvement of steric factors in the decelerating effect of (strept)avidin, we performed photoinactivation experiments with gA2XB, a biotinylated analogue of gramicidin A with a shorter linker arm (consisting of two aminocaproyl groups). Figure 6 shows the photoinactivation kinetics of gA2XB recorded before (curve 1) and after (curve 2) the addition of 20 nM Stv. The

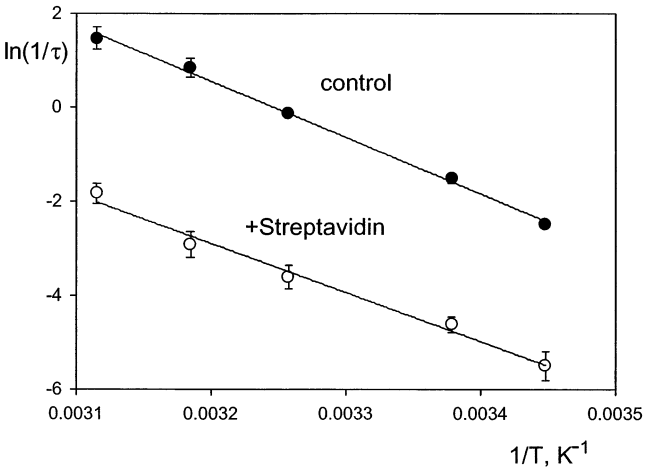

FIGURE 5: Arrhenius plot of the temperature dependence of gA5XB photoinactivation kinetics in the control (●) and in the presence of 20 nM Stv at both sides of the BLM (○).

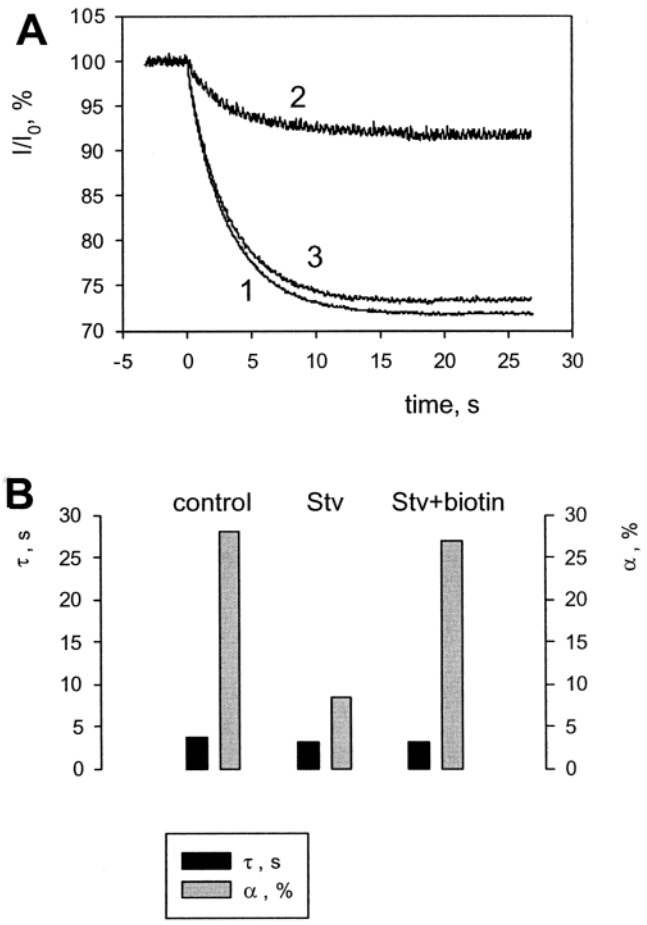

FIGURE 6: (A) Time courses of the decrease in the gA2XB-mediated current (I) across a BLM after a flash of visible light (at time zero) in the presence of 1 μM $AlPcS_3$ before (curve 1) and after the addition of 20 nM Stv (curve 2). Curve 3 was recorded in the presence of 20 μM biotin which was added to the bathing solutions on both sides of the BLM after the addition of streptavidin. The normalized values of the current (I/I_0) are plotted vs time (t). (B) Bar plot of the characteristic time (τ) and the relative amplitude [$\alpha = (I_0 - I_\infty)/I_0$] of the photoinactivation calculated from the curves presented in panel A. The initial value of the current (I_0) was approximately 1 μA. The BLM voltage was 50 mV. The solution was the same as that described in the legend of Figure 3.

control kinetics measured in the absence of Stv were fitted well by a monoexponential curve with a characteristic time (τ) of 3.1 s. The addition of Stv caused a substantial reduction of the relative amplitude of gA2XB photoinactivation (α), whereas τ remained unaltered. Remarkably, the Stv-induced decrease in α was removed by the addition of excess biotin (20 μM) to the bathing solutions (curve 3). These results clearly show that Stv binds to channel-forming gA2XB molecules embedded in the membrane, though this binding, in contrast to the interaction with gA5XB, does not lead to deceleration of the gA2XB photoinactivation kinetics. As observed previously (*29*), avidin also does not produce the decelerating effect on gA2XB kinetics. The reduction of the photoinactivation amplitude (α) suggests that the binding of Stv to gA2XB causes a decrease in the concentration of reactive oxygen species in the vicinity of the target (gA2XB) molecules, thereby protecting gA2XB molecules from the attack of reactive oxygen species.

DISCUSSION

We have hypothesized previously (*31*) that the great deceleration of the photoinactivation kinetics resulting from the interaction of (strept)avidin with a long linker biotinylated gramicidin (gA5XB) is due to the formation of the long-lived double-conductance channels, resembling the double-barreled channels observed by Goforth et al. (*41*) with covalently linked gramicidin analogues. Recently, a theoretical model has been proposed that explains the extremely long lifetimes of linked gramicidin channels by membrane-mediated elastic interactions between individual channels (*42*). To examine the role of biotin binding affinity in the streptavidin−gA5XB interaction, we measured single-channel activity and the macroscopic current induced by gA5XB in the presence of streptavidin mutants with reduced affinities for biotin. Stv-F120, like Stv, induced both the appearance of the double-conductance state in the gA5XB single-channel traces (Figure 1) and the tremendous deceleration of the gA5XB photoinactivation kinetics (Figure 3).

This result looks surprising if one takes into account the fact that the biotin binding affinity of Stv-F120 in solution is 6−7 orders of magnitude lower than that of Stv. However, a more striking result was obtained with Stv-A23D27, the affinity of which is further reduced by approximately 5 orders of magnitude. This mutant exerted a noticeable deceleration of the gA5XB photoinactivation kinetics (Figure 3) measured at a high density of gA5XB channels, though it was unable to induce double-conductance channels in single-channel experiments. The enhancement of interaction by increasing the surface density of receptors can be explained well within the framework of the bivalent binding model proposed previously (*31*). According to this model, the double-conductance channel arises from the bivalent binding of streptavidin molecules to gA5XB at both sides of the BLM that leads to cross-linking of two gA5XB channels. Thus, a new tandem channel comprising a pair of synchronously operating channels is formed. This model is based on the general assumption that usual gramicidin channels represent transmembrane dimers (*43*−*45*).

Apparently, the bivalent binding requires a rather high affinity for biotin, and this is the reason the streptavidin mutant with the lowest biotin binding affinity was inefficient in eliciting the double-conductance state in single-channel traces of gA5XB. On the other hand, Stv-A23D27 did bind

to gA5XB, because fast fluctuations of the single-channel current, normally preceding the opening of the double-conductance channels with Stv and Stv-F120, were also observed upon addition of Stv-A23D27 (Figure 2). These bursts are likely to result from the monovalent binding of Stv-A23D27 to gA5XB, with a single biotin-binding site on the tetrameric protein being occupied by the biotin group of gA5XB, in contrast to the bivalent mode of binding, in which two binding sites on streptavidin are occupied simultaneously by biotins belonging to a pair of gA5XB molecules. Termination of the bursts can be ascribed to the release of biotin groups of gA5XB molecules from binding sites of streptavidins or dissociation of transmembrane dimers of gA5XB bound to streptavidins. The former explanation seems more likely, because the average total duration of the bursts depended essentially on the streptavidin mutant that was used and correlated qualitatively with the biotin binding affinity. Fast fluctuations were observed only upon the addition of Stv and its mutants at both sides of a BLM. This fact proves that the bursts are associated with the formation of Stv−gA5XB−gA5XB−Stv complexes, where two streptavidin molecules are located at the opposite sides of the membrane.

To explain why Stv-A23D27, the mutant with an extremely low biotin binding affinity, induced the appearance of the long-lived channel state at the high density of gA5XB, one can assume that the interaction of the protein with gA5XB involves some kind of membrane−protein interaction. As shown in ref *46*, Stv interacts, with a substantial affinity, with a phosphatidylcholine monolayer even in the absence of biotin groups. A similar phenomenon was observed by us for fluorescein-labeled Stv that binds nonspecifically to a horizontal DPhPC bilayer (data not shown) by using a fluorescence microscope with a setup similar to that described in refs *47* and *48*. Thus, the formation of the double-conductance channels might involve initial, nonspecific binding of Stv-A23D27 to a lipid bilayer, followed by the binding to biotin groups of gA5XB molecules. The nonspecific binding of Stv-A23D27 should increase its local concentration on the membrane, allowing the protein to bind to gA5XB, despite its very low affinity for biotin. By taking into account the fact that the lateral area per lipid molecule in a BLM is $\sim$0.6 nm^2 (*49*) and assuming from the data of ref *46* that at least 1% of lipid molecules is involved in the nonspecific binding of Stv-A23D27 to a lipid bilayer, we can estimate the local surface concentration of the nonspecifically bound protein to be on the order of 10^{12} molecules/cm^2 ($\cong 10^{-12}$ mol/cm^2). This surface density corresponds to a local volume concentration of $\sim$3 mM, assuming that the mean distances in the volume are the same as on the surface. At this local concentration, Stv-A23D27, bound nonspecifically to the membrane, could bind efficiently to gA5XB despite its very low biotin binding affinity. Such initial nonspecific binding to the membrane should play a minimal, if any, role in the binding of Stv and Stv-F120 to gA5XB, since these proteins have sufficiently high biotin binding affinities. This is supported by the experimental result showing that the double-conductance channel state was formed at very low concentrations of these proteins (Table 1). The low efficacy of biotin in removing this long-lived state of gA5XB channels with Stv-A23D27, as compared to that with Stv and Stv-F120 (Figure 4), may also be explained by the contribution of the nonspecific binding of Stv-A23D27 to the formation of the double-conductance channels.

Examination of gA5XB single-channel traces in the presence of streptavidin (*31*) has revealed that both the opening and closing of the double-conductance state proceed via a transient substate with a conductance similar to the standard single-channel conductance of gA5XB. This indicates that the double-conductance channel closing represents successive dissociation of two transmembrane dimers forming the tandem channel. This is likely to account for the similarity between the activation energy derived from the temperature dependence of τ_2 (the exponential factor of the slow phase of photoinactivation observed after the addition of Stv) and the activation energy obtained from the temperature dependence of τ in the absence of streptavidin (Figure 5).

The data on the interaction of streptavidin with gA2XB channels are readily explained by the monovalent binding model. These data do not support the bivalent binding interaction, which likely does not occur due to the steric hindrance caused by the short linker arm of gA2XB. The monovalent binding of Stv to gA2XB appeared to induce only the reduction of the relative amplitude (α) of photoinactivation (Figure 6) and the fast fluctuations of the single-channel current, observed previously (*31*). The fact that the decrease in α was removed by the addition of excess free biotin confirms that this effect resulted from the binding of Stv to gA2XB. Apparently, the monovalent nature of Stv−gA2XB binding may be governed by structural factors. In particular, a certain spatial arrangement of biotinylated gramicidins bound to the same streptavidin tetramer, which is required for the formation of two neighboring transmembrane dimers (the tandem channel), may be severely hindered with the short linker channel former.

In summary, this work provides evidence that supports the bivalent binding of streptavidin to biotinylated gramicidin as the mechanism of tandem channel formation. The occurrence of the tandem gramicidin channels induced by the addition of streptavidins exhibits a strong dependence on their biotin binding affinity and the length of a linker arm between a biotin group and the C-terminus of gramicidin. The results of this study indicate that direct interaction of streptavidins with a lipid bilayer may facilitate their specific binding to biotin groups on the membrane.

ACKNOWLEDGMENT

We are grateful to F. Separovic and A. Anastasiadis (University of Melbourne) for the generous gift of biotinylated gramicidins and to A. G. Tonevitsky, I. I. Agapov, and N. S. Melik-Nubarov (Moscow State University) for helpful discussions.

REFERENCES

1. Akeson, M., Branton, D., Kasianowicz, J. J., Brandin, E., and Deamer, D. W. (1999) Microsecond time-scale discrimination among polycytidylic acid, polyadenylic acid, and polyuridylic acid as homopolymers or as segments within single RNA molecules, *Biophys. J. 77*, 3227−3233.
2. Howorka, S., and Bayley, H. (2002) Probing distance and electrical potential within a protein pore with tethered DNA, *Biophys. J. 83*, 3202−3210.
3. Mrksich, M., Grunwell, J. R., and Whitesides, G. M. (1995) Biospecific adsorption of carbonic anhydrase to self-assembled monolayers of alkanethiolates that present benzenesulfonamide groups on gold, *J. Am. Chem. Soc. 117*, 12009−12010.

4. Perez-Luna, V. H., O'Brien, M. J., Opperman, K. A., Hampton, P. D., Lopez, G. P., Klumb, L. A., and Stayton, P. S. (1999) Molecular recognition between genetically engineered streptavidin and surface bound biotin, *J. Am. Chem. Soc. 121*, 6469−6478.
5. Zhao, S., and Reichert, W. M. (1992) Influence of biotin lipid surface density and accessibility on avidin binding to the tip of an optical fiber, *Langmuir 8*, 2785−2791.
6. Zhao, S. L., Walker, D. S., and Reichert, W. M. (1993) Cooperativity in the binding of avidin to biotin-lipid-doped Langmuir−Blodgett films, *Langmuir 9*, 3166−3173.
7. Zhang, X., and Moy, V. T. (2003) Cooperative adhesion of ligand−receptor bonds, *Biophys. Chem. 104*, 271−278.
8. Bayley, H., and Cremer, P. S. (2001) Stochastic sensors inspired by biology, *Nature 413*, 226−230.
9. Cornell, B. A., Braach-Maksvytis, V. L., King, L. G., Osman, P. D., Raguse, B., Wieczorek, L., and Pace, R. J. (1997) A biosensor that uses ion-channel switches, *Nature 387*, 580−583.
10. Lucas, W. S., and Harding, M. M. (2000) Detection of DNA via an ion channel switch biosensor, *Anal. Biochem. 282*, 70−79.
11. Hirano, A., Wakabayashi, M., Matsuno, Y., and Sugawara, M. (2003) A single-channel sensor based on gramicidin controlled by molecular recognition at bilayer lipid membranes containing receptor, *Biosens. Bioelectron. 18*, 973−983.
12. Futaki, S., Fukuda, M., Omote, M., Yamauchi, K., Yagami, T., Niwa, M., and Sugiura, Y. (2001) Alamethicin-leucine zipper hybrid peptide: a prototype for the design of artificial receptors and ion channels, *J. Am. Chem. Soc. 123*, 12127−12134.
13. Zhang, Y., Futaki, S., Kiwada, T., and Sugiura, Y. (2002) Detection of protein−ligand interaction on the membranes using C-terminus biotin-tagged alamethicin, *Bioorg. Med. Chem. 10*, 2635−2639.
14. Cornell, B. A., Braach-Maksvytis, V. L., King, L. G., Osman, P. D., Raguse, B., Wieczorek, L., and Pace, R. J. (1999) The gramicidin-based biosensor: a functioning nano-machine, *Novartis Found. Symp. 225*, 231−249.
15. Wilchek, M., and Bayer, E. A. (1990) Introduction to avidin−biotin technology, *Methods Enzymol. 184*, 5−13.
16. Sano, T., Vajda, S., Reznik, G. O., Smith, C. L., and Cantor, C. R. (1996) Molecular engineering of streptavidin, *Ann. N.Y. Acad. Sci. 799*, 383−390.
17. Stayton, P. S., Freitag, S., Klumb, L. A., Chilkoti, A., Chu, V., Penzotti, J. E., To, R., Hyre, D., Le Trong, I., Lybrand, T. P., and Stenkamp, R. E. (1999) Streptavidin−biotin binding energetics, *Biomol. Eng. 16*, 39−44.
18. Hyre, D. E., Amon, L. M., Penzotti, J. E., Le Trong, I., Stenkamp, R. E., Lybrand, T. P., and Stayton, P. S. (2002) Early mechanistic events in biotin dissociation from streptavidin, *Nat. Struct. Biol. 9*, 582−585.
19. Sano, T., and Cantor, C. R. (1995) Intersubunit contacts made by tryptophan 120 with biotin are essential for both strong biotin binding and biotin-induced tighter subunit association of streptavidin, *Proc. Natl. Acad. Sci. U.S.A. 92*, 3180−3184.
20. Chilkoti, A., Tan, P. H., and Stayton, P. S. (1995) Site-directed mutagenesis studies of the high-affinity streptavidin-biotin complex: contributions of tryptophan residues 79, 108, and 120, *Proc. Natl. Acad. Sci. U.S.A. 92*, 1754−1758.
21. Sano, T., Vajda, S., Smith, C. L., and Cantor, C. R. (1997) Engineering subunit association of multisubunit proteins: a dimeric streptavidin, *Proc. Natl. Acad. Sci. U.S.A. 94*, 6153−6158.
22. Reznik, G. O., Vajda, S., Sano, T., and Cantor, C. R. (1998) A streptavidin mutant with altered ligand-binding specificity, *Proc. Natl. Acad. Sci. U.S.A. 95*, 13525−13530.
23. Klumb, L. A., Chu, V., and Stayton, P. S. (1998) Energetic roles of hydrogen bonds at the ureido oxygen binding pocket in the streptavidin−biotin complex, *Biochemistry 37*, 7657−7663.
24. Freitag, S., Le Trong, I., Chilkoti, A., Klumb, L. A., Stayton, P. S., and Stenkamp, R. E. (1998) Structural studies of binding site tryptophan mutants in the high-affinity streptavidin−biotin complex, *J. Mol. Biol. 279*, 211−221.
25. Laitinen, O. H., Airenne, K. J., Marttila, A. T., Kulik, T., Porkka, E., Bayer, E. A., Wilchek, M., and Kulomaa, M. S. (1999) Mutation of a critical tryptophan to lysine in avidin or streptavidin may explain why sea urchin fibropellin adopts an avidin-like domain, *FEBS Lett. 461*, 52−58.
26. Qureshi, M. H., Yeung, J. C., Wu, S. C., and Wong, S. L. (2001) Development and characterization of a series of soluble tetrameric and monomeric streptavidin muteins with differential biotin binding affinities, *J. Biol. Chem. 276*, 46422−46428.
27. Marttila, A. T., Hytonen, V. P., Laitinen, O. H., Bayer, E. A., Wilchek, M., and Kulomaa, M. S. (2003) Mutation of the important Tyr-33 residue of chicken avidin: functional and structural consequences, *Biochem. J. 369*, 249−254.
28. Suarez, E., Emmanuelle, E. D., Molle, G., Lazaro, R., and Viallefont, P. (1998) Synthesis and characterization of a new biotinylated gramicidin, *J. Pept. Sci. 4*, 371−377.
29. Rokitskaya, T. I., Antonenko, Y. N., Kotova, E. A., Anastasiadis, A., and Separovic, F. (2000) Effect of avidin on channel kinetics of biotinylated gramicidin, *Biochemistry 39*, 13053−13058.
30. Futaki, S., Youjun, Z., and Sugiura, Y. (2001) Detecting a tag on a channel opening: blockage of the biotinylated channels by streptavidin, *Tetrahedron Lett. 42*, 1563−1565.
31. Rokitskaya, T. I., Kotova, E. A., and Antonenko, Y. N. (2003) Tandem gramicidin channels cross-linked by streptavidin, *J. Gen. Physiol. 121*, 463−476.
32. Green, N. M. (1975) Avidin, *Adv. Protein Chem. 29*, 85−133.
33. Green, N. M. (1990) Avidin and streptavidin, *Methods Enzymol. 184*, 51−67.
34. Separovic, F., Barker, S., Delahunty, M., and Smith, R. (1999) NMR structure of C-terminally tagged gramicidin channels, *Biochim. Biophys. Acta 1416*, 48−56.
35. Anastasiadis, A., Separovic, F., and White, J. (2001) Synthesis of deuterated aminocaproyl linkers, *Aust. J. Chem. 54*, 747−750.
36. Straessle, M., and Stark, G. (1992) Photodynamic inactivation of an ion channel: gramicidin A, *Photochem. Photobiol. 55*, 461−463.
37. Rokitskaya, T. I., Antonenko, Y. N., and Kotova, E. A. (1993) The interaction of phthalocyanine with planar lipid bilayers: photodynamic inactivation of gramicidin channels, *FEBS Lett. 329*, 332−335.
38. Kunz, L., Zeidler, U., Haegele, K., Przybylski, M., and Stark, G. (1995) Photodynamic and radiolytic inactivation of ion channels formed by gramicidin A: oxidation and fragmentation, *Biochemistry 34*, 11895−11903.
39. Rokitskaya, T. I., Antonenko, Y. N., and Kotova, E. A. (1996) Photodynamic inactivation of gramicidin channels: a flash-photolysis study, *Biochim. Biophys. Acta 1275*, 221−226.
40. Rokitskaya, T. I., Block, M., Antonenko, Y. N., Kotova, E. A., and Pohl, P. (2000) Photosensitizer binding to lipid bilayers as a precondition for the photoinactivation of membrane channels, *Biophys. J. 78*, 2572−2580.
41. Goforth, R. L., Chi, A. K., Greathouse, D. V., Providence, L. L., Koeppe, R. E., and Andersen, O. S. (2003) Hydrophobic coupling of lipid bilayer energetics to channel function, *J. Gen. Physiol. 121*, 477−493.
42. Partenskii, M. B., Miloshevsky, G. V., and Jordan, P. C. (2003) Stabilization of ion channels due to membrane-mediated elastic interaction, *J. Chem. Phys. 118*, 10306−10311.
43. Koeppe, R. E., and Andersen, O. S. (1996) Engineering the gramicidin channel, *Annu. Rev. Biophys. Biomol. Struct. 25*, 231−258.
44. Andersen, O. S., Apell, H. J., Bamberg, E., Busath, D. D., Koeppe, R. E., Sigworth, F. J., Szabo, G., Urry, D. W., and Woolley, G. A. (1999) Gramicidin channel controversy: the structure in a lipid environment, *Nat. Struct. Biol. 6*, 609−612.
45. Cross, T. A., Arseniev, A., Cornell, B. A., Davis, J. H., Killian, J. A., Koeppe, R. E., Nicholson, L. K., Separovic, F., and Wallace, B. A. (1999) Gramicidin channel controversy: revisited, *Nat. Struct. Biol. 6*, 610−612.
46. Blankenburg, R., Meller, P., Ringsdorf, H., and Salesse, C. (1989) Interaction between biotin lipids and streptavidin in monolayers: formation of oriented two-dimensional protein domains induced by surface recognition, *Biochemistry 28*, 8214−8221.
47. Serowy, S., Saparov, S. M., Antonenko, Y. N., Kozlovsky, W., Hagen, V., and Pohl, P. (2003) Structural proton diffusion along lipid bilayers, *Biophys. J. 84*, 1031−1037.
48. Brutyan, R. A., DeMaria, C., and Harris, A. L. (1995) Horizontal 'solvent-free' lipid bimolecular membranes with two-sided access can be formed and facilitate ion channel reconstitution, *Biochim. Biophys. Acta 1236*, 339−344.
49. Cornell, B. A., Middlehurst, J., and Separovic, F. (1980) The molecular packing and stability within highly curved phospholipid bilayers, *Biochim. Biophys. Acta 598*, 405−410.

BI034984R